Finite Element Analysis on Rapid Prototyping Pattern with Different Internal Structure for Investment Casting

M.N. Hafsa[1], M. Ibrahim[2], S. Sharif[3], O.M.F. Marwah[4] And S. Sulaiman[5]

[1](Faculty of Mechanical and Manufacturing Engineering, Universiti Tun Hussein Onn Malaysia, Batu Pahat, Johor, Malaysia
[2](Faculty of Mechanical and Manufacturing Engineering, Universiti Tun Hussein Onn Malaysia, Batu Pahat, Johor, Malaysia
[3](Faculty of Mechanical Engineering, Universiti Teknologi Malaysia, Skudai, Johor, Malaysia
[4](Faculty of Mechanical and Manufacturing Engineering, Universiti Tun Hussein Onn Malaysia, Batu Pahat, Johor, Malaysia
[5](Faculty of Mechanical and Manufacturing Engineering, Universiti Tun Hussein Onn Malaysia, Batu Pahat, Johor, Malaysia

ABSTRACT

Manufacturing a metal product with complex geometry usually will related to Investment Casting (IC) process as the process has the highest capability to deliver the intended objective. But producing the wax pattern for the process has already consumes half of the time of overall process. Rapid Prototyping (RP) is considered to be a solution as it capable to reduce the time in a large margin. Compared to wax patterns traditionally made for IC, RP patterns mainly built from polymer based material. Polymer may react differently than wax when it comes to the burnout process which is a critical part in IC that determines the quality of the final cast product. By considering both strength and collapsibility, cube pattern with different internal structure designs were developed using SolidWorks software and analysis by ANSYS software. All designs were tested for total deformation and equivalent Von Misses stress within the temperature range from room temperature of 27ºC up to 700ºC. The result from the simulation indicates that most of the shell cracking takes place in the initial steps of the burnout stage which is before the glass transition temperature of thermosetting patterns. Shells cracking are strongly related to the internal structure of the Multi-Jet Modeling (MJM) patterns. The study shows the possibility and places of mould cracking during the burnout process.

Keywords – Acrylate, Finite Element Analysis, Investment Casting, Multi-Jet Modeling, Rapid Prototyping

I. INTRODUCTION

Since the introduction of RP technology, researches have actively been conducted. Besides application in producing end product, RP technology could potentially be implemented into other manufacturing process. Nowadays, polymer pattern manufactured using RP has been identified to be a good candidate to replace the traditional wax pattern in IC process. With RP capability to produce a complex shape within short time while having good dimensional accuracy, production lead time in IC process could significantly be reduced [1].

IC was before a definite choice if part with complex feature and good accuracy to be cast. However, IC require a wax pattern to be produce beforehand and it consume almost half of the total process time to produce the wax pattern. Replacing the wax pattern making process with RP is a lot of time saving. There are two commercial RP methods, Selective Laser Sintering (SLS) and Fused Deposition Modeling (FDM) which are capable to produce wax model that can directly be used in IC [2,3,4,5,6,7].

Though, early attempts of using RP model as the sacrificial pattern for IC did not turn out pretty well as the solid model, it encounter quite significant thermal expansion during the burn out process thus causing the ceramic shell to crack [6]. Aside from that, there have been studies on the causes of shell cracking during pattern burnout in IC [2,8,9,10]. It occur on the pattern produced of non wax material such ABS, epoxy, and acrylic [4,6,11]. From a study, a simple hollow geometry was proven to be generally better compared to solid pattern [1,11]. The idea was supported with a series of conducted studies comparing a hollow and a solid pattern within temperature below glass transition temperature of epoxy resin that lead to a conclusion, shell cracking will not occur if the glass transition temperature of the epoxy is lower than ceramic shell cracking temperature [3,10,12].

In order for the ceramic shell to remain intact, the pattern had to be much weaker to allow it to disintegrate easily. Due to that reason, pattern with quasi hollow design are hoped to be able to flows out of the shell easily during burn out process [6]. Experimental procedure involving high temperature and delicate specimen could be quite tedious, thus numerical model should provide similar result with

lesser effort. A numerical model can be used to determine by computer simulation if the ceramic shell is likely to crack during burn out process in IC. The models are useful in developing a computer-aided engineering tool for the design of the internal structures of the pattern [10]. The objective of this study is to determine the thermally induced stresses during the pattern burnout process using finite element analysis and the use of this analysis for the design of the MJM pattern's internal structure.

II. METHODOLOGY

During the burn out process in IC, the polymer pattern made from RP will be heated until it melt and collapse inside the ceramic shell, before its flows out of the ceramic shell leaving vacant space for molten metal to be poured in. As polymer pattern have different properties compared to traditional wax pattern, it may react differently during the burn out process.

Four different internal structures of cube (30mm) were developed using SolidWorks software as shown in Fig. 1a. Fig. 1b shows the internal structures of cube which are consist of hollow, square, cross, and hatch pattern. Aside from the polymer cube design, the ceramic shell must also be developed. The ceramic shell model is simply to enclose the entire polymer cube with the exception of one surface.

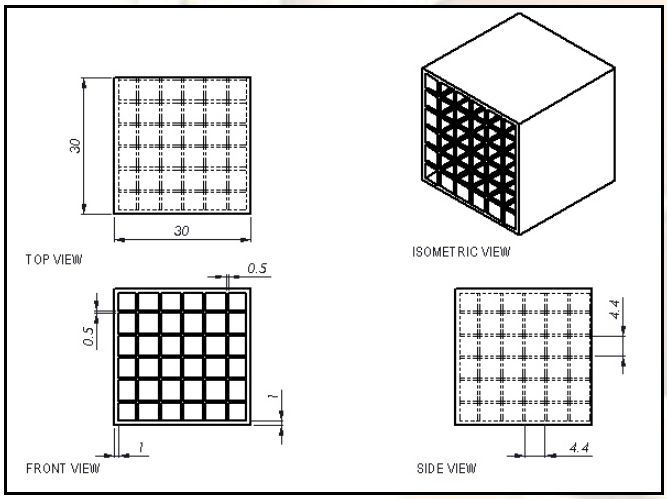

(a)

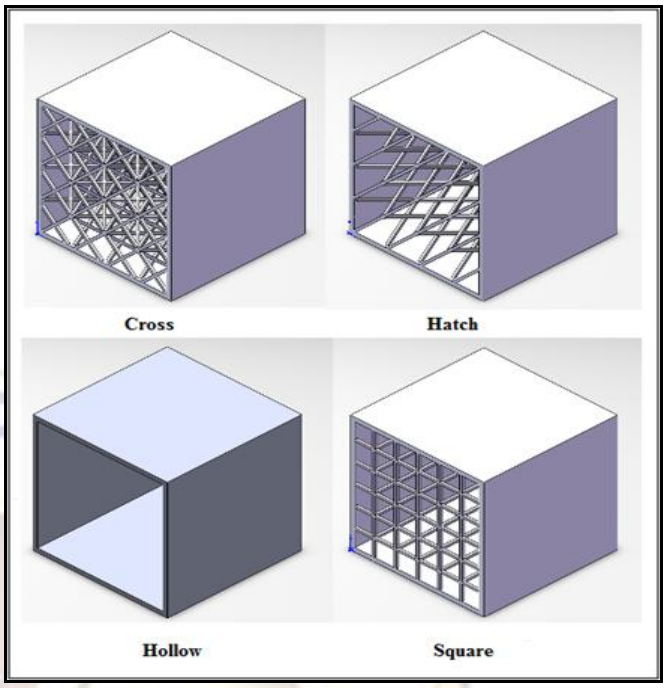

(b)

Fig. 1. (a) Cube technical drawing (b) Internal structure pattern design inside the cube

The study will involve a numerical study and a mechanical testing to support the result from the numerical study. In order to perform the numerical studies using ANSYS Software, the tensile stress and the tensile modulus of the Visijet® SR200 acrylate material were required beforehand for the software to be able to perform the simulation. Dog-bone-shape specimens for tensile test were made using MJM technique according to ASTM D638 (refer Fig. 2). The tensile sample was tested using a Universal Testing Machine with a 10kN load cell. The test was conducted with constant speed of 5 mm/min. The nominal overall length, thickness and width of the narrow section were 165mm, 3.2mm and 13mm, respectively.

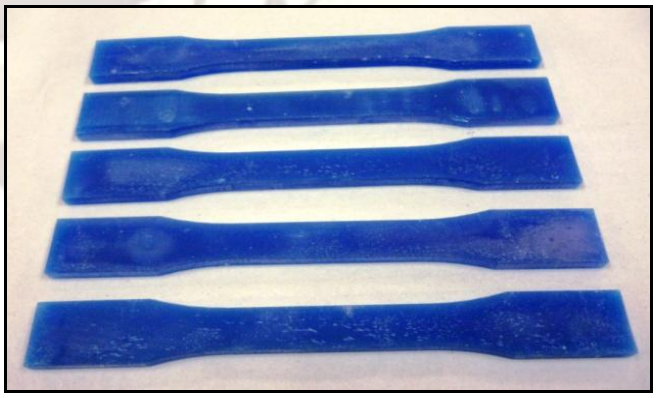

Fig. 2. Dog-bone-shape specimens for tensile test

For the numerical studies, Finite Element (FE) based software was used to investigate the relation between elastic stress concentration patterns

and buckling patterns observed in the experiments. 3D models with different internal structure in the form of cube (30mm) geometry. A dimension of the internal link (wall thickness 1mm, structure link 0.5mm) and thickness of ceramic shell (7mm) are the same for all internal structure patterns, without any change during numerical analysis.

The CAD modeling was undertaken on SolidWorks software. From CAD, an IGES file format has been generated for FE analysis. A cube specimen with 7mm thickness ceramic shell was analyzing by ANSYS finite element simulation. The FE mesh used in this study is a manipulated between fine, medium or course for span angle center and cell size. It was setting to be a high definition of smoothing. Table 1 indicates the result.

Table 1. Contact pressure, interface of acrylic pattern and ceramic shell, results by ANSYS FEA

Model	Mesh size	Number of elements	Max contact pressure [GPa]
Ceramic + Hollow	Course	3608	8.830
	Medium	12083	12.091
	Fine	33737	15.323
Ceramic + Cross	Course	36986	8.767
	Medium	49785	10.890
	Fine	58761	15.229
Ceramic + Hatch	Course	20652	7.518
	Medium	36171	10.292
	Fine	58188	13.088
Ceramic + Square	Course	24625	8.790
	Medium	35815	11.807
	Fine	59862	15.199

The temperature uniformity in the webbed pattern and the ceramic is assumed. Virtually it is difficult to keep the temperature uniform during continuous heating of the web structure. The temperature is changed from 20ºC to 700ºC with 20ºC rise for each step and kept long enough to reach the desired uniform temperature.

III. MATERIAL PROPERTIES ANALYSIS

Stress-strain curves in Fig. 3 were plotted based on the the apparent stress (MPa) and strain (%) values determined by dividing the load value by the initial cross sectional area of each tensile test specimen and the deformation values by the initial specimen. The value of Young' modulus taken at the point 0.809mm stroke and 300.72N force. The tensile strength and Young's modulus of the Visijet® SR200 acrylate base material were measured to be 24.23MPa and 550.47, respectively.

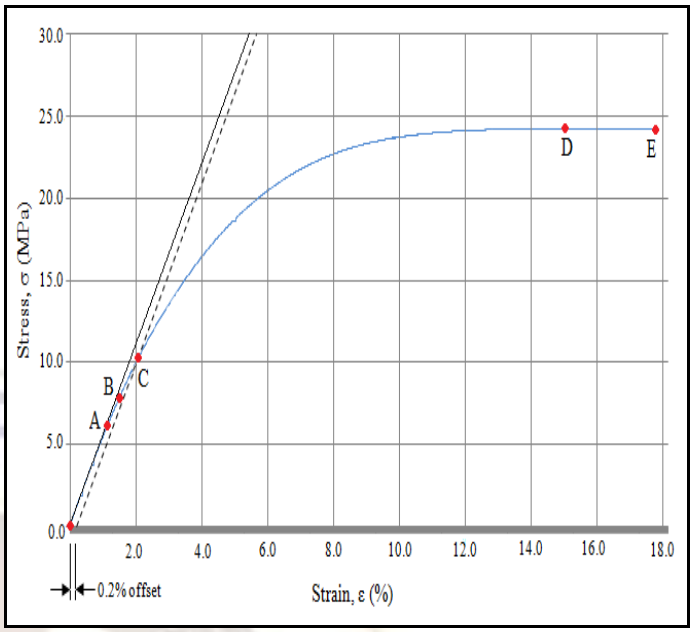

Fig. 3. Stress-strain curves of Visijet® SR200

acrylate base material produced by MJM technique From point O-A, curve is linear which material obey Hooke's Law. The material regains its original dimension when applied force is removed. In this region, the specimen behaves like an elastic body. The value of Modulus of Elasticity taken at the slope at the end point A-O. Stress and strain not porportional at point A-B. The point B is known as elastic limit. Until this point the specimen can came back to original shape.

Point C is determined by 0.2% off-set method. It found by drawing a parallel line to the elastic region (Point O-A). It is a commonly used method to determine the yield strength. In this stage, the specimen does not regain its original dimension. Point D is an ultimate tensile strength of the material. Beyond this point, it is the maximum stress that the material can withstand while being stretched before breaking. At the point E, fracture occurs. Since the point D-E is close, Visijet® SR200 Acrylic material is known as brittle [13,14].

The tensile test was performed after the specimen were fabricated using ProJet™ SD3000 3-D Printer machine. The specimen preparation was done similar to the master pattern. The specimen was not made using injection moulding process since it will not have the same material properties as the material will be much denser. Similar to other part produced by RP, the specimen also occur to have the staircase effect and some voids.

IV. TOTAL DEFORMATION AND STRESS – TEMPERATURE ANALYSIS

Deformation of Visijet® SR200 acrylate material can be seen from the finite element analysis result as shown in Fig.

4. The red marking resembles the area which the deformations were maximums while the blue marking resembles the area with the minimum deformation during the burnout process. From the result, it could be identified that the ceramic shell would not crack as the deformation rate was at the minimum level. The deformation is changing with respect of temperature.

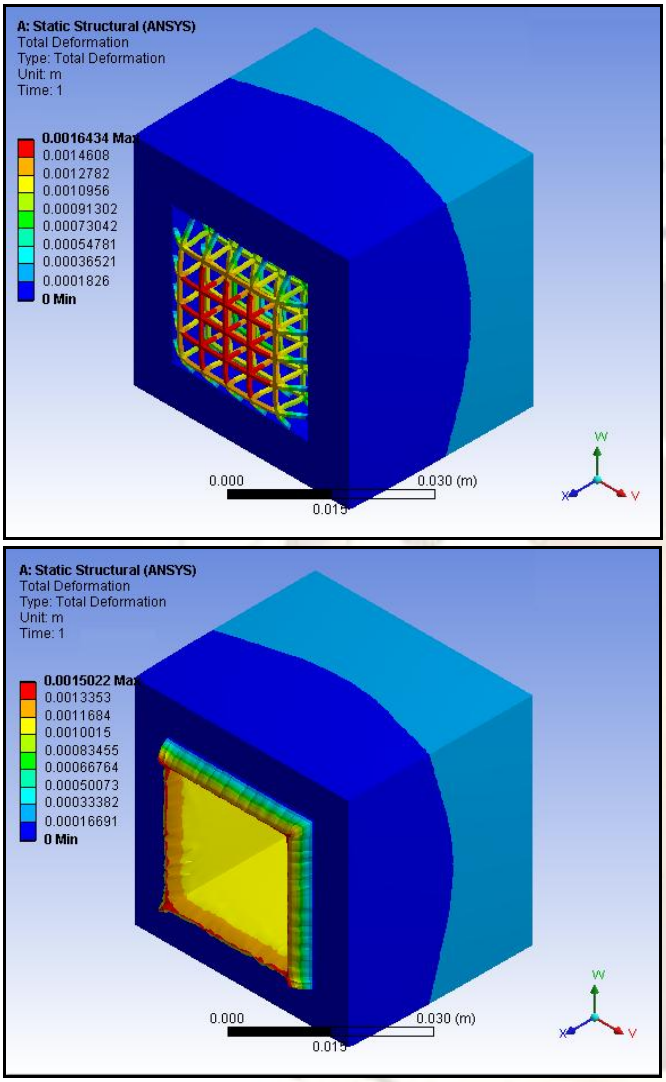

Fig. 4. Total deformation obtained from the finite element analysis for square and hollow internal pattern structure

The graph in Fig. 5 shows that at the maximum temperature of 700 ºC, the cross internal structure has the highest total deformation of 0.20481mm followed by square internal pattern with 0.16434mm and hollow internal pattern with 0.15022mm. The hatch internal pattern was significantly lower than the other three with 0.00035m of total deformation. For part with hatch internal structure, the mould has the tendencies to crack.

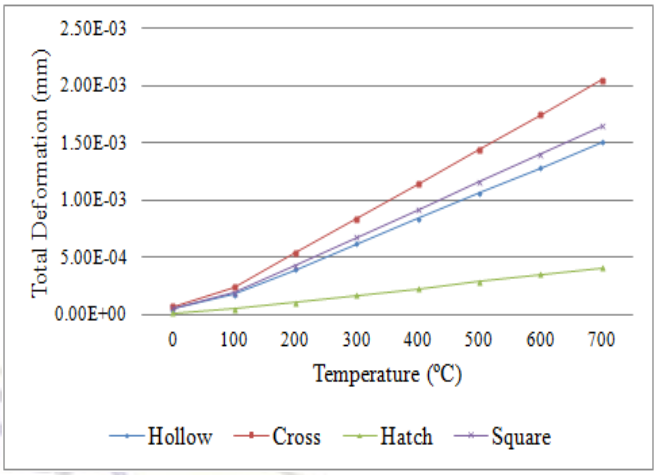

Fig. 5. Total deformation against temperature for different internal structure

Plastic deformation and pore deformation are limited when applied with high strain rate compressive load, suggesting that the formation of cracks which are in line with buckling bands could be associated with elastic stress concentration patterns in each structure [15]. Stress softening at the onset of plastic deformation is well known phenomenon in foam mechanics and is associated with pore deformation and shear band formation.

From the graph of equivalent stress versus temperature (see Fig. 6), the maximum equivalent stress at 700ºC for hollow, cross, and square internal pattern are closely similar with the value ranging of 15.323GPa, 15.229GPa, and 15.199GPa respectively. Again, the value for hatch internal pattern was significantly lower with the equivalent stress of 13.088GPa. The FEM is employed to calculate the distribution of temperature and stress in the different internal structure of MJM specimen. Since the solidification part is cooled rapidly, the model tends to be deformed and cracked due to the thermal stress.

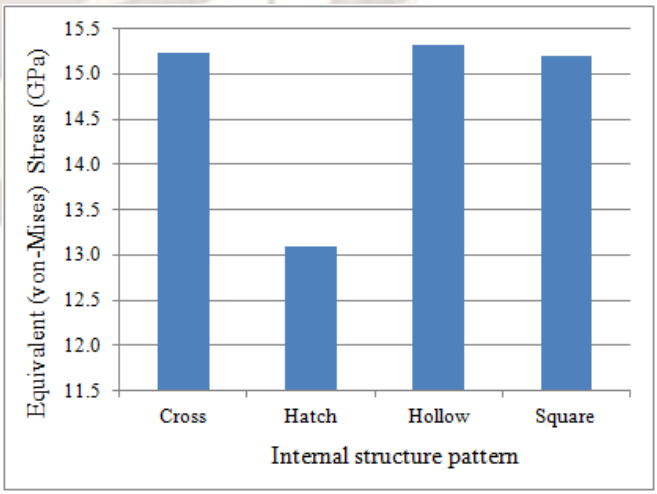

Fig. 6. Graph of equivalent stress against temperature for different internal structure

When an IC shell with MJM epoxy pattern inside, is in a furnace during burnout process, it is subjected to high temperature rise, thermal expansion and large strain. Since the different of CTE's of epoxy and IC is more than one order magnitude, the acrylic pattern can consider as a stress on the ceramic shell [6,16]. During the pattern burnout process, the inner acrylate pattern expands more than the outer ceramic shell. As a result, there exists contact pressure between the ceramic shell and epoxy pattern. The inner acrylate pattern is subjected to a compressive load, and the outer ceramic shell is subjected to a tensile load.

V. CONCLUSION

The tensile test was performed to obtain the properties of the material. The value is very important to obtain a good simulation result. For pattern drainage and collapsibility, properties obtained from testing were used to perform the FEA. The tensile strength and Modulus of Elasticity of the Visijet® SR200 acrylic material were measured to be 24.23MPa and 550.47MPa, respectively. Visijet® SR200 Acrylic material is known as brittle and suitable for being as sacrificial pattern for IC. The MJM patterns as thermally expendable patterns in shell IC are to address the issue of pattern collapsibility. The pattern must be able to collapse without affecting the ceramic shell. The FEA simulated the total deformation and thermal stress generated during burnout process in IC with different internal structure of MJM acrylic material. The maximum equivalent stress at 700ºC is hollow internal pattern structure with the value 15.323GPa. The cross internal structure has the highest total deformation of 0.20481mm. The total deformation value of part with cross internal structure was the highest since there were much more acrylate material to react with the temperature increase. Hatch internal structure seems to be significantly weaker compared to the others due to the lack of vertical strength. Even so, the hollow and square pattern seems to cope pretty well among the other designs.

VI. ACKNOWLEDGEMENTS

The authors would like to thank the Faculty of Mechanical & Manufacturing Engineering in Universiti Tun Hussein Onn Malaysia (UTHM) and the Faculty of Mechanical Engineering in Universiti Teknologi Malaysia (UTM) for their financial support and facilitating in this research programme.

REFERENCES

[1] W.S.W. Harun, S. Sharif, M.H. Idris and K. Kardirgama, Characteristic studies of collapsibility of ABS patterns produced from FDM for investment casting. *Material Research Innovations, 13 (3)*, 2009, 340-343.

[2] P.M. Dickens, R. Stangroom, and M. Greul, Conversion of RP models to investment castings. *Rapid Prototyping Journal, 1 (4)*, 1995, 4-11.

[3] R. Hague and P.M. Dickens, Stresses created in ceramic shells using Quickast models. Proceedings of the Solid Freeform Fabrication Symposium. H. Marcus. University of Texas at Austin, Austin, 1995, 242-252.

[4] J.C. Ferreira and A. Mateus, A numerical and experimental study of fracture in RP stereolithography patterns and ceramic shells for investment casting, *Journal of Materials Processing Technology, 134*, 2003, 135-144.

[5] W.S.W. Harun, S. Safian, and M.H. Idris, Evaluation of ABS patterns produced from FDM for investment casting process. *Computational Method and Experiments in Materials Characterisation IV*, 2009, 319-328.

[6] Y. Norouzi, S. Rahmati, and Y. Hojjat, A novel lattice structure for SL investment casting patterns. *Rapid Prototyping Journal, 15*, 2009, 255-263.

[7] M.F.M. Omar, S. Sharif, M. Ibrahim, H. Hehsan, M.N.M. Busari, and M.N. Hafsa, Evaluation of direct rapid prototyping pattern for investment casting. *Advanced Materials Research, 463-464*, 2012, 226-233.

[8] P. Blake, O. Baumgardner, L. Haburay, and P. Jacobs, Creating complex precision metal parts using QuickCast. *SME Conference on Rapid Prototyping and Manufacturing*, 1994.

[9] P.F. Jacobs, Rapid prototyping and manufacturing fundamentals of stereolithography. *SME Publication*, 1992.

[10] W.L. Yao and M.C. Leu, Analysis of shell cracking in investment casting with laser stereolithography patterns. *Rapid Prototyping Journal, 5(1)*, 1999, 12-20.

[11] M.N. Hafsa, M. Ibrahim, S. Sharif, M.F.M. Omar, and M.A. Zainol, Evaluation of different internal structure and build orientation for multi-jet modeling process. *Applied Mechanics and Materials, 315*, 2013, 587-591.

[12] R. Hague and P.M. Dickens, Requirements for the successful autoclaving of the stereolithography models in the investment casting process. *National Conference on Rapid Prototyping and Tooling Research, Buckinghamshire College*, 1996, 77-92.

[13] G. Ryder, B. Ion, G. Green, D. Harrison, and B. Wood, Rapid design and manufacture

tools in architecture. *Automotion in Construction*, *11*, 2002, 279-290.

[14] R. Su, G. M. Campbell, and S.K. Boyd, Establishment of an architecture - specific experimental validation approach for finite element modeling of bone by rapid prototyping and high resolution computed tomography. *Medical Engineering & Physics*, *29*, 2007, 480-490.

[15] R. B. Patil and V. Yadava, Finite element analysis of temperature distribution in single metallic powder layer during metal laser sintering. *International Journal of Machine Tools and Manufacture*, *47*, 2007, 1069-1080.

[16] R. Hague, G. D'Costa, and P. M. Dickens, Structural design and resin drainage characteristics of QuickCast 2.0. *Rapid Prototyping Journal*, *7 (2)*, 2001, 66-72.